Cys114-Linked Dimers of Transthyretin Are Compatible with Amyloid Formation[†,‡]

Anders Karlsson, Anders Olofsson, Therese Eneqvist,[§] and A. Elisabeth Sauer-Eriksson*

Umeå Centre for Molecular Pathogenesis, Umeå University, SE-901 87 Umeå, Sweden

Received April 29, 2005; Revised Manuscript Received August 1, 2005

ABSTRACT: The Tyr114Cys substitution in the human plasma protein transthyretin leads to a particularly aggressive form of familial amyloidotic polyneuropathy. In a previous study we demonstrated that ATTR Tyr114Cys forms intermolecular disulfide bonds, which partly impair fibril formation and result in a more amorphous morphology. Apart from the introduced cysteinyl group in position 114, the native sequence contains one cysteine located at position 10. To deduce the role of intermolecular disulfide bridging in fibril formation we generated and characterized the TTR Cys10Ala/Tyr114Cys double mutant. Our results suggest that an intermolecular cysteine bridge at position 114 enhances the exposure of cysteine 10, thereby facilitating additional intermolecular cysteine assemblies. We also purified a disulfide-linked dimeric form of TTR Cys10Ala/Tyr114Cys, which was recognized by the anti-TTR amyloid-specific monoclonal antibody MAb (39−44). Moreover, this dimeric molecule can form protofibrils indistinguishable from the fibrils formed under reducing conditions, as judged by atomic force microscopy. Assuming that both molecules of the dimer are part of the core of the fibril, the assembly is incompatible with a preserved native or near-native dimeric interphase. Our findings raise the question of whether TTR-amyloid architecture is indeed the result of one highly stringent assembly of structures or if different fibrils may be built from different underlying structures.

Transthyretin (TTR)[1] is a 55 kDa homotetrameric protein mainly expressed in the liver and choroid plexus of the brain. It is secreted into plasma and cerebrospinal fluid, where it functions as a transport protein for the thyroid hormones thyroxine (T4) and triiodothyronine (T3). TTR also transports holo-retinol binding protein (holo-RBP) in plasma, thereby preventing it from renal excretion. TTR is implicated in three amyloid disorders. Familial amyloidotic polyneuropathy (FAP) is an autosomal dominant disorder caused by one of over 80 known single-point mutations in TTR. The accumulation of amyloid in FAP is usually associated with peripheral neuropathy, resulting in disrupted motor, sensory, and autonomic functions (for reviews see refs *1*−*3*). Variant TTR proteins are also involved in the hereditary familial amyloidotic cardiopathy (FAC) (*4*), while the wild-type protein is implicated in the late-onset senile systemic amyloidosis (SSA) (*5*, *6*).

Amyloid formation and deposition are complex processes yet to be fully understood. Evidence from numerous in vitro studies shows that amyloid formation is a multistep process involving amyloidogenic intermediates (for reviews see refs *7*−*12*). For TTR, most studies suggest that its misassembly is caused through tetramer dissociation followed by partial monomer denaturation (*13*−*17*). Other studies suggest that transthyretin amyloid fibrils seem to assemble from oligomeric protein building blocks rather than restructured monomers (*18*−*23*). To prevent fibril formation, kinetic stabilization of the native tetrameric conformation of TTR by high-affinity binding of small ligands has proved to be the most successful approach (*24*−*26*).

Various post-translational modifications of Cys10, the sole cysteine residue in the wild-type TTR (wtTTR) monomers, have been observed in ex vivo TTR protein variants (*27*, *28*). In particular, cysteinylation occurs at increased levels in TTR purified from FAP patients (*29*, *30*). Disulfide-bond linked ATTR Val30Met protein has also been reported from ex vivo amyloid from patients (*31*). In vitro studies have shown that these modifications have implications in the stability of the protein, i.e., they increase the propensity for aggregation (*32*−*35*). Recently, three lines of transgenic mice, expressing ATTR Val30Met, wtTTR, and an artificial Cys-free mutant TTR Cys10Ser/Val30Met, were generated and used to study the role of Cys10 in amyloidogenesis (*36*). Histochemical investigation showed that deposition of amyloid could only be derived from the ATTR Val30Met mice, indicating that Cys10 plays a crucial role in TTR Val30Met amyloidogenesis in vivo. Presumably, the methionine for valine substitution induces changes in the hydrogen-bonding pattern of the Cys10 side chain, resulting in an increased

[†] This study was supported by the Swedish Research Science Council (K2004-03X-13001-06A, K2004-03EF-15196-01A, K2004-03B-15003-01A), the patients' association FAMY/AMYL, M. Bergvalls foundation, Kempe foundation, Hjärnfonden, and Socialstyrelsen.

[‡] Atomic coordinates of the transthyretin variant TTR C10A/Y114C structure have been deposited in the Research Collaboratory for Structural Bioinformatics (RCSB) with the accession code 1IJN.

* To whom correspondence should be addressed. E-mail: liz@ucmp.umu.se. Phone: +46-90-7856782. Fax: +46-90-778007.

[§] Present address: Department of Biochemistry and Biophysics, Stockholm University, SE-106 91 Stockholm, Sweden.

[1] Abbreviations: TTR, transthyretin; AFM, atomic force microscopy; ATTR, in vivo amyloidogenic TTR; BME, β-mercaptoethanol; ECL, enhanced chemiluminiscence; FAC, familial amyloidotic cardiomyopathy; FAP, familial amyloidotic polyneuropathy; IPTG, isopropyl thiogalactopyranoside; PBS, phosphate buffered saline, PEG, polyethylene glycol; rms, root-mean-square; SSA, senile systemic amyloidosis; TBS, Tris buffered saline; wtTTR, wild-type TTR.

10.1021/bi050795s CCC: $30.25
Published on Web 09/08/2005

propensity of the sulfur atom to form other bonds (*36*). In support, recent data from studies in vitro showed that disulfide modifications of residue Cys10 decreased the stability and increased the amyloidogenicity of TTR variants (*35*).

The TTR variant Tyr114Cys was first described in a Japanese population with a particularly severe form of FAP (*37*, *38*), and was later identified in Dutch patients (*39*). The carriers of this mutation show initial symptoms in their thirties with a life expectancy of about 10 years after onset of the disease. The ATTR Tyr114Cys variant can be purified as a native tetramer, as determined by size-exclusion chromatography (*40*). However, the protein readily forms fibrils and the reaction is significantly enhanced at higher temperatures. Under nonreducing conditions, fibril formation is partly impaired by formation of intermolecular disulfide bonds resulting in a more amorphous precipitate (*40*). The crystal structure of ATTR Tyr114Cys (*40*) shows few structural differences compared to the wild-type protein; however, β-mercaptoethanol (BME) is associated with the substituted residue Cys114 indicating a tendency of this residue to form disulfide bonds. Cys10 is found in a more buried position than in the wild-type structure; it seems to be hindered sterically from forming disulfide bonds. Taken all together, these results show that disulfide-bond formation is heavily involved in the formation and morphology of ATTR Tyr114Cys aggregates (*40*).

The aim of the present study was to further investigate the role of Cys10 in TTR amyloid formation, and in particular its involvement in the aggregation of ATTR Tyr114Cys, by characterizing the double substitution mutant TTR Cys10Ala/Tyr114Cys. In the course of the investigation we were able to isolate a disulfide-linked dimeric form of TTR Cys10Ala/Tyr114Cys. This dimeric variant could be heat-induced to form protofibrils morphologically similar to those formed by the ATTR Tyr114Cys variant. Interestingly, we also found that the disulfide-linked dimeric form was recognized by the TTR-amyloid specific monoclonal antibody MAb (39−44). The data suggest that while a cysteine residue at position 10 is not necessary for protofibril formation of ATTR Tyr114Cys in vitro, its presence nonetheless enhances the propensity of the mutant to form Cys114-linked disulfide bonds.

MATERIAL AND METHODS

Cloning, Expression, and Purification of Recombinant Proteins. The TTR Cys10Ala/Tyr114Cys double mutant was generated using PCR site-directed mutagenesis as described previously (*40*). Competent *Escherichia coli* BL21 (DE3) cells were transformed and plated onto LB agar plates containing 50 μg/mL carbenicillin. The colonies were harvested and grown at 37 °C in LB medium containing 100 μg/mL carbenicillin. When the OD_{600nm} reached 0.8, the cells were induced with 0.2 mM isopropyl thiogalactopyranoside (IPTG) for 3 h and subsequently harvested by centrifugation. Following resuspension in buffer A (20 mM Tris-HCl pH 7.5, and 100 mM NaCl), the cells were frozen in liquid nitrogen and stored at −80 °C.

The wtTTR and TTR variants were purified using the same protocol. The cells were thawed at room temperature and lysed by sonication. Insoluble debris was pelleted by centrifugation at 37000*g* for 35 min at 4 °C. The supernatant was loaded onto a Q-sepharose Fast Flow anion-exchange column and eluted with a linear NaCl gradient (0.1−1.0 M NaCl) in 20 mM Tris-HCl, pH 7.5. Fractions confirmed by SDS−PAGE to contain TTR were pooled and dialyzed overnight against buffer A and then loaded onto a MonoQ 10/100 HR anion-exchange column equilibrated with the same buffer. Proteins were eluted with a linear NaCl gradient (0.1−1.0 M) employing 20 mM Tris-HCl pH 7.5. Fractions estimated to contain >80% pure TTR were pooled and concentrated to 5.0 mg/mL using a Centriprep YM-10 and then loaded onto a HiLoad 16/60 Superdex 75 PG gel filtration column equilibrated in buffer B (20 mM Tris-HCl pH 7.2, and 100 mM NaCl). Protein purity was assessed by SDS−PAGE, and TTR fractions of an estimated purity of >95% were pooled, frozen in liquid nitrogen, and stored at −80 °C.

Aggregation and Fibril Formation of TTR Variants. Heat-induced aggregation of wild-type TTR and the amyloidogenic mutants ATTR Val30Met, ATTR Tyr114Cys, and TTR Cys10Ala/Tyr114Cys was assessed by native PAGE and SDS−PAGE using Homogeneous 20 Phast gels. The proteins were diluted to 0.5 mg/mL in buffer B and incubated at 37 °C or 55 °C for 96 h under nonreducing or reducing conditions. The reducing condition included 144 mM BME. Before the SDS−PAGE analysis, protein samples were boiled for 10 min in loading buffer containing 2.5% SDS prior to application on the gel. For the reduced samples, the loading buffer included 0.7 M BME.

For protofibril visualization we used atomic force microscopy (AFM) using the protocol described by Eneqvist et al. (*40*), but with the scan rate ranging from 0.75 to 1.5 Hz.

Crystallization, Data Collection, Structure Determination, and Refinement. Diffraction quality crystals of TTR Cys10Ala/Tyr114Cys were grown in 5 days at room temperature to $0.1 \times 0.1 \times 0.3$ mm^3 by the hanging-drop, vapor-diffusion method. The crystals belong to space group $P2_12_12$ isomorphous to the wild-type protein (*41*, *42*) and the Tyr114Cys mutant (*40*). The total drop volume was 10 μL, containing a 4:1 (v/v) mixture of the reservoir; 36−40% polyethylene glycol 550 mono methyl ether, 100 mM sodium citrate, pH 5.0, 100 mM ammonium sulfate, 14.4 mM BME, and protein solution; 3.0 mg/mL protein in 50 mM Tris-HCl, pH 7.5. We did not obtain crystals without BME.

Diffraction data were collected at 100 K from a single crystal supported in a cryo loop (*43*) using synchrotron radiation at the wavelength 0.934 Å on a 160 mm MAR-research CCD detector at ESRF, Grenoble, France. Data processing and structure determination were done as described previously (*40*). Refinement was done using conjugate gradient minimization and simulated annealing, as implemented in CNS, alternated with manual rebuilding of the model using the program O (*44*). The structure was further refined with the program REFMAC, part of the CCP4 program package (*45*) using the maximum likelihood residual, anisotropic scaling, bulk-solvent correction, and atomic displacement parameter refinement (*46*). Details of the data collection, quality of data, and refinement statistics are shown in Table 1.

Purification and Analysis of the Disulfide-Linked TTR Cys10Ala/Tyr114Cys. TTR Cys10Ala/Tyr114Cys protein (4 mg/mL) was incubated at 55 °C for 96 h. The aggregated

Table 1: Data Collection, Refinement, and Structural Statistics

(A) Data Collection[a]	
space group	$P2_12_12$
cell dimensions *a*, *b*, *c* (Å)	43.15, 85.24, 64.80
resolution (Å)	20−1.7 (1.76−1.70)
no. of observations	212406
no. of unique reflections	26695 (2479)
completeness (%)	98.1 (93.0)
$I/\sigma(I)$	24.5 (4.7)
R_{merge}[b] (%)	3.4 (22.2)
(B) Refinement	
resolution range used in refinement (Å)	19.9−1.7
no. of reflections in the working set	23858
no. of reflections in the test set	2665
R-factor[c] for the working set (%)	20.4
R_{free}[d] for the test set (%)	23.7
no. of residues included in the model	10−125 (A), 10−124 (B)
no. of water molecules	216
occupancy of BME, linked to Cys114 (A/B monomers)	0.80/0.40
oxidized form in channel (A/B monomers)	0.30/0.40
mean temperature factor (Å^2)	19.7
Ramachandran plot (most favored, additional allowed, generously allowed) (%)	90.0/9.5/0.5
rms deviations[e]	
for bond lengths (Å)	0.008
for bond angles (deg)	1.27
for torsion angles in period 1 (deg)	3.87
for torsion angles in period 3 (deg)	15.3
(C) Structure	
rms deviations	
compared to wild-type TTR A/B[f] (Å)	0.431/0.266
for monomer A vs monomer B[f] (Å)	0.653
dimer−dimer interface area (Å^2)	2460

[a] Values in parentheses are for the highest resolution shell. [b] $R_{merge} = \sum_h\sum_i|I_{ih} - \langle I_h\rangle|\sum_h\sum_i\langle I_h\rangle$ where $\langle I_h\rangle$ is the mean intensity of the *i* observations of reflection *h*. [c] *R*-factor $= \sum||F_{obs}| - |F_{calc}||/\sum|F_{obs}|$, where $|F_{obs}|$ and $|F_{calc}|$ are the observed and calculated structure factor amplitudes, respectively. Summation includes all reflections used in the refinement. [d] $R_{free} = \sum||F_{obs}| - |F_{calc}||/\sum|F_{obs}|$, evaluated for a randomly chosen subset of 10% of the diffraction data not incuded in the refinement. [e] Root-mean-square deviation from ideal values. [f] The main chain atoms of residues Cys10−Asn98 and Arg104−Thr123 were used in the calculations.

protein was solubilized in Tris-buffered urea (6 M urea, 20 mM Tris-HCl, pH 7.2) for 18 h at 4 °C, followed by centrifugation at 20800*g* for 50 min. The supernatant was loaded on a HiPrep 16/60 Sephacryl S-100 HR gel filtration column equilibrated in the solubilization buffer. Fractions containing TTR Cys10Ala/Tyr114Cys dimers, as confirmed by nonreducing and reducing SDS−PAGE, were pooled and refolded by dialysis against 5 L of buffer B for 18 h at 4 °C. The refolded protein was further purified on a HiLoad 16/60 Superdex 75 PG gel filtration column equilibrated in buffer B. The dimer-containing fractions were pooled, frozen in liquid nitrogen, and stored at −80 °C.

Fibrils of purified TTR Cys10Ala/Tyr114Cys dimers were obtained by heat incubation at 55 °C for 96 h. The initial dimer concentration was 0.5 mg/mL in buffer B. AFM studies were performed as described (*40*) with the scan rate ranging from 0.75 to 1.9 Hz. The dimeric form of the mutant was maintained in the protofibrils as confirmed by SDS−PAGE analyses at reducing and nonreducing conditions.

Immunoprecipitation and Western Blot Analyses of TTR Variants. Freshly thawed preparations of wtTTR as well as the TTR variants Val30Met, Tyr114Cys, and Cys10Ala/Tyr114Cys, and the purified dimeric form of the Cys10Ala/Tyr114Cys protein after heat-incubation, were immunoprecipitated using an anti-TTR amyloid monoclonal antibody (*47*). Fifty microliters of protein G sepharose (Amersham Biosciences) was added along with 20 μg of MAb (39−44) for 15 min at room temperature. The protein-G antibody complex was washed several times, through repeated centrifugation with 50 mM Tris-HCl, pH 7.5 and 0.05% (v/v) Tween-20, the final wash including the Tris buffer only. Twenty micrograms of each TTR-variant was subsequently added to the antibody and incubated for 15 min at room temperature. The samples were washed as described above, and resuspended in phosphate-buffered saline (PBS), pH 7.4. After a short spin, the pellets were dissolved in 100 μL of SDS−PAGE loading buffer (without BME), separated by nonreducing SDS−PAGE, using Phast Homogeneous 20 gels, and transferred to nitrocellulose membranes (Hybond-P pure, Amersham), and the membrane was blocked with 5% skimmed milk. Immunodetection was performed with polyclonal rabbit anti-TTR antibodies and horseradish peroxidase conjugated anti-rabbit immunoglobulins (Amersham). Detection was performed with enhanced chemiluminiscence (ECL, Pierce).

RESULTS

Analysis of Disulfide-Bond Formation in TTR Cys10Ala/Tyr114Cys. We analyzed and compared wtTTR, ATTR Val30Met, ATTR Tyr114Cys, and TTR Cys10Ala/Tyr114Cys to study the effects of disulfide-bond formation on aggregation in vitro. We employed a strategy where the proteins were incubated for 96 h at medium (37 °C) or high (55 °C) temperatures in the presence and absence of the reducing agent BME, followed by analysis on native PAGE and SDS−PAGE under reducing and nonreducing conditions (Figure 1A−D). Both wtTTR and ATTR Val30Met were virtually unaffected by high-temperature incubation. Both proteins migrated as tetramers in the nonreducing and reducing native PAGE (Figure 1A and Figure 1C, respectively). In the nonreducing SDS−PAGE (Figure 1B), they migrated as monomers with a small fraction of the proteins forming dimers. The ATTR Tyr114Cys variant on the other hand migrated in four discrete bands in the nonreducing PAGE experiment (Figure 1A, lane 3a). These bands correspond to the native tetrameric form of the protein as well as to three other forms. Interestingly, the migration pattern of the Cys10Ala/Tyr114Cys double mutant also showed the presence of the same four bands after incubation at 37 °C (Figure 1A, lane 2b). When high concentrations of BME were added to Cys10Ala/Tyr114Cys and Tyr114Cys, they migrated as tetramers, verifying that the oligomeric structures observed are formed by S−S bonds (Figure 1C). These bands are most likely composed of multimers of Cys114−Cys114 linked dimers; i.e., dimers, native or non-native tetramers, small amounts of hexamers, and octamers. For the double mutant, which has only one cysteine residue, the formation of higher multimers must involve dimer−dimer interactions not based on S−S bonds. After incubation at medium temperature (37 °C), the migration pattern of Tyr114Cys shifts to display four major bands on a native gel (Figure 1A, lane 3b). This implies that Cys10 is also involved in disulfide-bond formation. Interestingly, the protein no longer seems to form

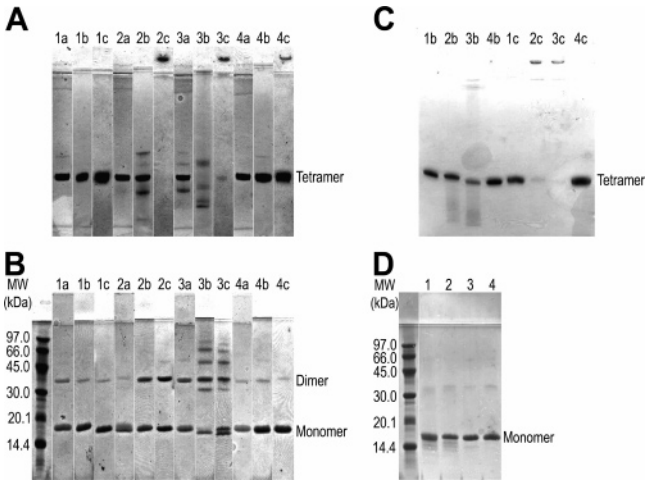

FIGURE 1: Analysis of TTR by PAGE: (A) nonreducing native PAGE, (B) nonreducing SDS−PAGE, (C) reducing native PAGE, and (D) reducing SDS−PAGE. The lanes contain samples of the four TTR variants: (1) ATTR Val30Met, (2) TTR Cys10Ala/Tyr114Cys, (3) ATTR Tyr114Cys, and (4) wtTTR. The lanes of each group represent the original protein preparations (freshly thawed) (a) and samples incubated for 96 h at 37 °C (b) and 55 °C (c), respectively. The migration pattern of nonincubated ATTR Tyr114Cys in nonreducing SDS−PAGE shows that it migrates as monomers and dimers, whereas incubation at 37 °C and 55 °C results in migration patterns displaying a ladder of bands, with molecular weights ranging from below tetramer size to large aggregates (Figure 1B, lane 3a−c). As expected, ATTR Tyr114Cys incubated at 55 °C migrated mostly as monomers in reducing SDS−PAGE (D, lane 3).

the regular tetrameric conformation at this point. After induction at the highest temperature, 55 °C, the Tyr114Cys and Cys10Ala/Tyr114Cys proteins are almost exclusively in a highly aggregated form, which barely enters the gel (lanes 2c and 3c). These high-molecular aggregates cannot be reduced with BME, which indicates that it is other interactions together with the disulfide bonds that cause these aggregates. The migration patterns of both proteins in nonreducing SDS−PAGE (Figure 1B, lanes 2b and 3a) verified that at least the initial aggregates were composed of dimers of disulfide-linked Cys114 residues. Disulfide-linked dimer formation of Tyr114Cys was however initiated at lower temperatures. As expected, all TTR variants, which had been incubated at 55 °C, migrated as monomers in reducing SDS−PAGE (Figure 1D).

Atomic force microscopy (AFM) analysis of TTR Cys10Ala/Tyr114Cys after incubation at high temperature (55 °C) showed the presence of protofibrils under both reducing (Figure 2A) and nonreducing conditions (Figure 2B). The purified sample of the disulfide-linked dimeric form of Cys10Ala/Tyr114Cys also formed protofibrils following incubation at 55 °C (Figure 2C). These fibrillar structures were morphologically similar to those formed in heat-incubated reduced Cys10Ala/Tyr114Cys and Tyr114Cys (*40*), and heat-incubated nonreduced Cys10Ala/Tyr114Cys. Immunoprecipitation and Western blot hybridization using an anti-TTR amyloid-specific monoclonal antibody showed that the fibrils are composed of TTR intermediates maintaining the amyloidogenic fold (Figure 3). SDS−PAGE analyses

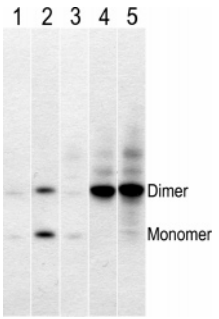

FIGURE 3: Immunoprecipitation and Western blot of TTR. TTR variants were precipitated using the TTR amyloid-specific monoclonal antibody MAb (39−44). Western blot of the precipitated protein indicated that ATTR Val30Met (lane 1) and wtTTR (lane 2), both incubated at 55 °C for 96 h, do not display the amyloid-characteristic epitope to any significant extent. This is in agreement with previous results (*47*). The tetrameric form of TTR Cys10Ala/Tyr114Cys (lane 3) did not react significantly with the MAb (39−44) antibody at room temperature, while the purified, disulfide-linked dimeric form reacted strongly with the antibody both before (lane 4) and after (lane 5) incubation at 55 °C for 96 h under nonreducing conditions.

under nonreducing and reducing conditions confirmed that the protofibrils formed by the purified Cys10Ala/Tyr114Cys dimers comprised disulfide-linked species (Figure 4).

The X-ray Crystallographic Structure of TTR Cys10Ala/Tyr114Cys. The atomic structure of TTR Cys10Ala/Tyr114Cys crystallized in the presence of BME was refined to 1.7 Å resolution. The structure is highly similar to wtTTR. Excluding the N- and C-terminal residues from superposition, root-mean-square (rms) deviations are 0.43 Å comparing the A monomers only, and 0.27 Å comparing the B monomers. These values are equivalent to structures of other TTR variants exhibiting the native fold (*42*). Residues situated in

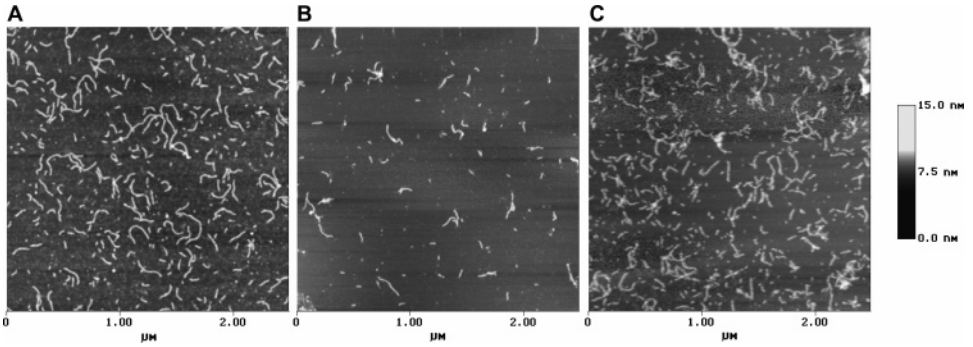

FIGURE 2: Fibrillization studies of recombinant TTR Cys10Ala/Tyr114Cys material in vitro. Equal amounts of protein were incubated with or without BME at 55 °C for 96 h to induce fibrillization. Visualization by atomic force microscopy (AFM) of (A) reduced and (B) nonreduced material. (C) Protofibrils formed by a purified disulfide-bonded dimeric form of TTR Cys10Ala/Tyr114Cys, which has been incubated at 55 °C for 96 h under nonreducing conditions.

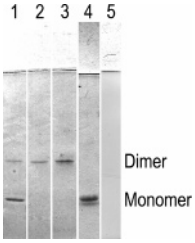

FIGURE 4: Characterization of a disulfide-bonded dimeric form of TTR Cys10Ala/Tyr114Cys by reducing and nonreducing SDS−PAGE. After the initial purification, the major part of the protein migrates as monomers, with a small fraction migrating as dimers (lane 1, see also Figure 1, lane 2a), indicating that this TTR variant, like wtTTR, is mostly tetrameric. After incubation at 55 °C, a dimeric species was purified at 4 °C (lane 2, see also Materials and Methods). As visualized by AFM, heat incubation at 55 °C induced fibril formation of the purified dimers (see Figure 2C). SDS−PAGE analyses of this material without BME (lane 3) and with BME (lane 4) confirmed the presence of S−S-linked dimers in the fibrils. Analysis on a native gel shows that these fibrils are not dissolved by the addition of BME (lane 5)

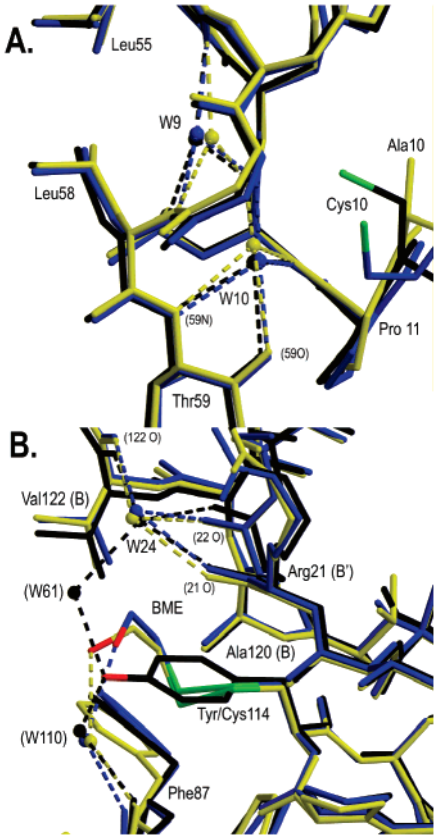

FIGURE 5: Structural alignment of wtTTR in black (PDB entry 1F41 (*42*)), ATTR Tyr114Cys in blue (PDB entry 1IIK (*40*)), and TTR Cys10Ala/Tyr114Cys in yellow. (A) Ala10 in monomer A. (B) Cys114 in monomer A.

the direct vicinity of Ala10 are virtually unaffected by the removal of the sulfur atom. If anything, a small shift of the position of residues Leu55−Phe64 can be observed. This shift of 0.5−0.6 Å positions the main chain of the latter residues away from β-strand A (Figure 5A).

The Tyr to Cys substitution at residue 114 is well defined in the electron density map. Similar to what we observed in the ATTR Tyr114Cys structure (*40*), Cys114 in the double mutant forms a disulfide bond to a BME molecule, to occupy roughly the same space as the tyrosine residue in the wild-type structure (Figure 5B). The occupancy of the BME molecules in the A and B monomers is 0.80 and 0.40, respectively.

Similarly to the ATTR Tyr114Cys protein, TTR Cys10Ala/Tyr114Cys binds two pairs of disulfide-linked BME molecules at its hormone-binding channel, one in each hormone-binding site. These oxidized BME molecules replace water molecules W28, W33, W35, and W36, observed in wtTTR (PDB 1F41 (*42*)). The occupancy of the BME molecules situated in the hormone-binding channel is rather low; 0.30 and 0.40 for the A and B monomers, respectively. The hydroxyl groups of the oxidized BME molecules form hydrogen bonds to the Oγ and Oγ1 atoms of Ser117 and Thr119, respectively, which probably stabilizes the tetrameric form of the protein.

DISCUSSION

In a previous study, we observed that aggregates, extracted from patients with the ATTR Tyr114Cys variant, exhibited two distinct morphologies: amyloid fibrils and disulfide-linked amorphous precipitates. Overexpressed and purified ATTR Tyr114Cys in vitro can form similar deposits by heat incubation under nonreducing and reducing conditions (*40*). To further investigate the role of disulfide bonds in this process, and in particular the role of Cys10, we introduced a Cys to Ala substitution into the Tyr114Cys variant. The TTR Cys10Ala/Tyr114Cys double mutant is thus unable to form oligomers linked by disulfide bonds of larger size than dimers.

PAGE migration pattern analyses were performed on heat-incubated TTR variants. As controls, we used wtTTR and ATTR Val30Met (Figure 1). The combined results from the native PAGE and the nonreducing SDS−PAGE suggested that identical disulfide-linked dimers are present in both the ATTR Tyr114Cys and the TTR Cys10Ala/Tyr114Cys material. However, in the latter, they are only induced by heat incubation. This implies that, in the early process of aggregation, i.e., when the proteins are largely native in their respective structures, only Cys114 is involved in disulfide-bond formation. Further evidence is found in the crystal structures of both ATTR Tyr114Cys (*40*) and TTR Cys10Ala/Tyr114Cys (this study) which showed high-affinity binding of BME molecules to Cys114. After heat induction at 55 °C, Cys10 also starts participating in disulfide-bond formation, resulting in more extensively cross-linked aggregates that become too big to enter the native gels. Since these aggregates cannot be dissolved by BME alone, yet are rich in disulfide-linked oligomers, their formation probably involves other interactions of hydrophobic or electrostatic nature. Atomic force microscopy of Cys10Ala/Tyr114Cys revealed protofibrils, but unlike the Tyr114Cys variant, these fibrils can also be formed under nonreducing conditions. This suggests that the amyloidogenic properties of ATTR Tyr114Cys are due to structural alterations conferred through the substitution at residue 114 rather than events involving Cys10. Intriguingly, Cys10 seems to play an important role in promoting S−S bond formation of Cys114 residues, viz., for the Cys10Ala/Tyr114Cys mutant, disulfide bonds formed only after heating at 37 °C, whereas for the Tyr114Cys mutant, they appeared at room temperature. In addition, Cys10 has been identified as a key residue in the amyloidogenesis of ATTR Val30Met (*36*).

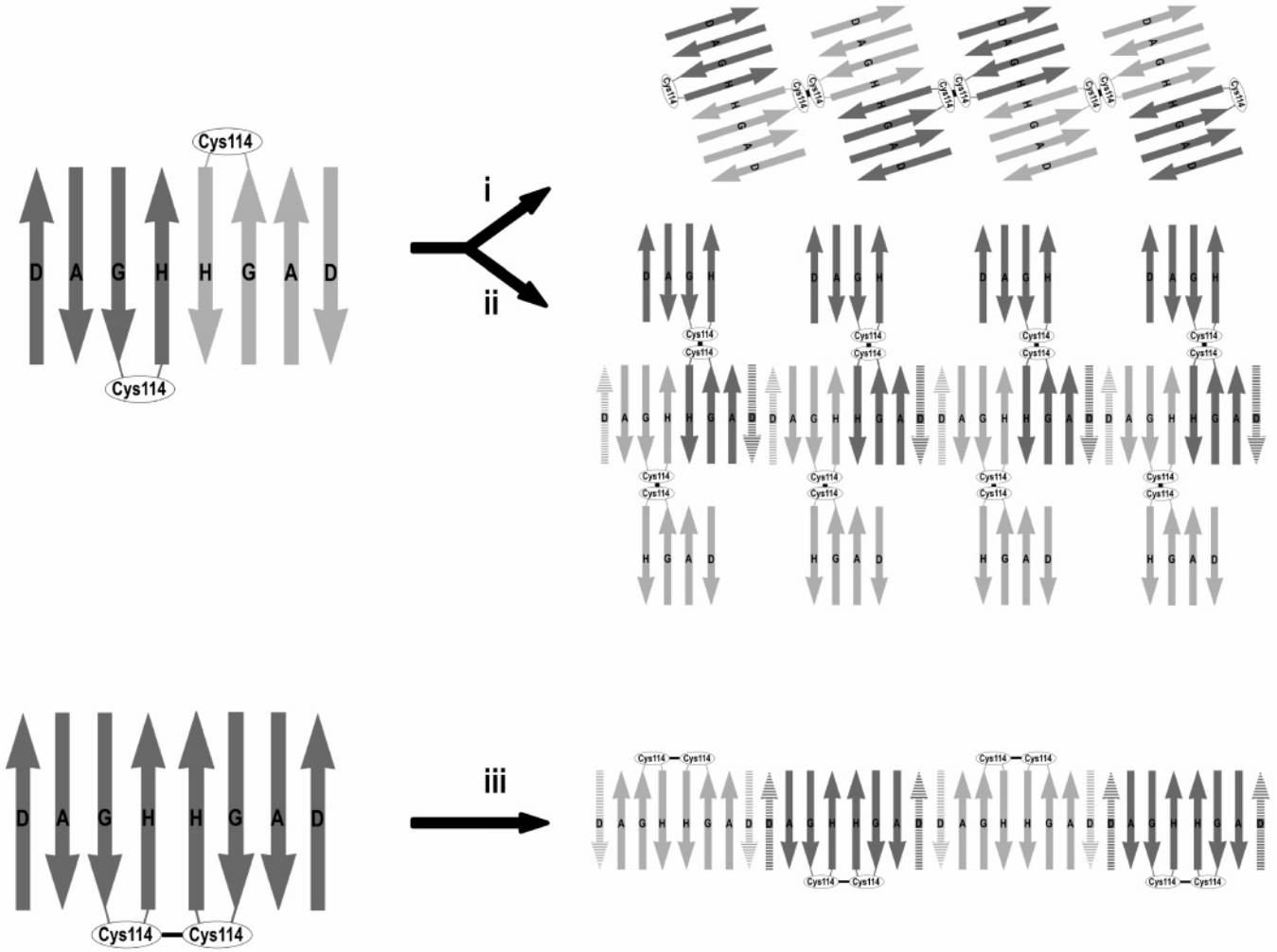

FIGURE 6: Plausible models for disulfide-bond mediated fibril formation of TTR Cys10Ala/Tyr114Cys. The figure illustrates two models of aggregation involving moderately denatured disulfide-linked "true" dimers that (i) aggregate through interactions between the Cys114 residues between two dimers or (ii) interact through the edge-strand region. Model iii shows a plausible fibril formed by "wrong" dimers of Cys10Ala/Tyr114Cys stabilized by intradimeric Cys114−Cys114 interactions, the wrong dimers being characterized by parallel H-strand H-strand interactions. β-Strand D is shadowed to indicate that it might be absent in the fibrillar structure (*18*, *19*, *21*). To improve clarity, identical S−S-linked dimers in the fibrillar structures are colored in light and dark gray.

The extent of disulfide-bonded oligomers observed in aggregated TTR Cys10Ala/Tyr114Cys led us to postulate that a disulfide-linked species might be an intermediate in the in vitro amyloid-formation process. A disulfide-linked dimeric sample of the Cys10Ala/Tyr114Cys variant was therefore isolated and found to form protofibrillar structures morphologically similar to those formed in vitro by ATTR Tyr114Cys (Figure 2). Since denaturing PAGE of the protofibrils resulted in a dimeric band only, we interpreted that to mean that the dimeric species is retained in the protofibrils (Figure 4, lane 3). As for the variants ATTR Tyr114Cys and TTR Cys10Ala/Tyr114Cys, the mature protofibril-like aggregates must be stabilized by interactions other than the intermonomeric disulfide bonds, since the fibrils are not dissolved by the addition of BME (Figure 4, lane 5).

Based on the structural and biochemical data, we propose that disulfide-bond formation in ATTR Tyr114Cys occurs sequentially. Initially the Cys114 residues form intermonomeric or interdimeric disulfide bonds. The partly buried position of Cys114 in the dimer−dimer interface suggests that tetramers in the native conformation must be structurally modified to sterically allow for Cys114−Cys114 interactions. As the monomers or dimers of Tyr114Cys become structurally altered or less ordered, the side chain of Cys10 becomes more available for disulfide-bond formation, which prevents fibril formation.

In TTR Cys10Ala/Tyr114Cys, a Cys114−Cys114 linked dimeric form of the protein adopts an amyloidogenic conformation recognized by MAb (39−44) and which readily assemblies as protofibrils. A previous study has shown that immature amyloid fibrils can be formed from a thiol-specific cross-linked dimeric form of TTR, suggesting that dimer interactions may be retained upon fiber formation (*18*). Based on this study and others, it has been suggested that nativelike dimers form the building blocks of the amyloid (*18*, *20*). There are several plausible mechanisms by which fibril formation of the dimeric form of TTR Cys10Ala/Tyr114Cys could occur. Dimers linked through Cys114−Cys114 residues can only form "wrong dimers", i.e., where the H-strands are positioned parallel rather than antiparallel with respect to each other. However, another possibility is that the Cys114−Cys114 linked dimer forms a nativelike dimer by reacting with another dimer (Figure 6). At this point it cannot be excluded that these dimer−dimer complexes can form nativelike tetrameric structures.

The intricate process of TTR amyloid formation seems to be even more complex than previously suspected. Studies have shown that immature fibrils form from monomeric structures (*48*), as well as from Cys114−Cys114 linked "wrong" dimers (the current study), Cys89−Cys96 linked nativelike dimers (*18*), and even truncated versions of the protein (*49*). This suggests that TTR-amyloid architecture, at least in vitro, is not a result of a highly stringent assembly and that fibrils may be built from different underlying protein structures.

ACKNOWLEDGMENT

We thank Dr. Uwe H. Sauer for his assistance with X-ray data collection and Terese Bergfors for critical reading of the manuscript.

REFERENCES

1. Saraiva, M. J. (1995) Transthyretin mutations in health and disease, *Hum. Mutat. 5*, 191−6.
2. Benson, M. D., and Uemichi, T. (1996) Transthyretin amyloidosis, *Amyloid: Int. J. Exp. Clin. Invest. 3*, 44−56.
3. Hamilton, J. A., and Benson, M. D. (2001) Transthyretin: a review from a structural perspective, *Cell. Mol. Life Sci. 58*, 1491−521.
4. Jacobson, D. R., Pastore, R. D., Yaghoubian, R., Kane, I., Gallo, G., Buck, F. S., and Buxbaum, J. N. (1997) Variant-sequence transthyretin (isoleucine 122) in late-onset cardiac amyloidosis in black Americans, *N. Engl. J. Med. 336*, 466−73.
5. Cornwell, G. G. d., Sletten, K., Johansson, B., and Westermark, P. (1988) Evidence that the amyloid fibril protein in senile systemic amyloidosis is derived from normal prealbumin, *Biochem. Biophys. Res. Commun. 154*, 648−53.
6. Westermark, P., Sletten, K., Johansson, B., and Cornwell, G. G. d. (1990) Fibril in senile systemic amyloidosis is derived from normal transthyretin, *Proc. Natl. Acad. Sci. U.S.A. 87*, 2843−5.
7. Harper, J. D., and Lansbury, P. T., Jr. (1997) Models of amyloid seeding in Alzheimer's disease and scrapie: mechanistic truths and physiological consequences of the time-dependent solubility of amyloid proteins, *Annu. Rev. Biochem. 66*, 385−407.
8. Kelly, J. W. (1998) The alternative conformations of amyloidogenic proteins and their multi-step assembly pathways, *Curr. Opin. Struct. Biol. 8*, 101−6.
9. Pepys, M. D. (1998) in *Immunological Diseases* (Samter, M., Ed.) pp 631−74, Little, Brown & Company, Boston.
10. Sipe, J. D., and Cohen, A. S. (2000) Review: History of the amyloid fibril, *Amyloid: Int. J. Exp. Clin. Invest. 130*, 88−98.
11. Koo, E. H., Lansbury, P. T., Jr., and Kelly, J. W. (1999) Amyloid diseases: abnormal protein aggregation in neurodegeneration, *Proc. Natl. Acad. Sci. U.S.A. 96*, 9989−90.
12. Rochet, J. C., and Lansbury, P. T., Jr. (2000) Amyloid fibrillogenesis: themes and variations, *Curr. Opin. Struct. Biol. 10*, 60−8.
13. Colon, W., and Kelly, J. W. (1992) Partial denaturation of transthyretin is sufficient for amyloid fibril formation in vitro, *Biochemistry 31*, 8654−60.
14. Lai, Z., Colón, W., and Kelly, J. W. (1996) The acid-mediated denaturation pathway of transthyretin yields a conformational intermediate that can self-assemble into amyloid, *Biochemistry 35*, 6470−82.
15. Redondo, C., Damas, A. M., and Saraiva, M. J. (2000) Designing transthyretin mutants affecting tetrameric structure: implications in amyloidogenicity, *Biochem. J. 348* (Part 1), 167−72.
16. Hammarström, P., Schneider, F., and Kelly, J. W. (2001) Trans-suppression of misfolding in an amyloid disease, *Science 293*, 2459−62.
17. Hammarström, P., Jiang, X., Hurshman, A. R., Powers, E. T., and Kelly, J. W. (2002) Sequence-dependent denaturation energetics: A major determinant in amyloid disease diversity, *Proc. Natl. Acad. Sci. U.S.A. 99* (Suppl. 4), 16427−32.
18. Serag, A. A., Altenbach, C., Gingery, M., Hubbell, W. L., and Yeates, T. O. (2001) Identification of a subunit interface in transthyretin amyloid fibrils: evidence for self-assembly from oligomeric building blocks, *Biochemistry 40*, 9089−96.
19. Serag, A. A., Altenbach, C., Gingery, M., Hubbell, W. L., and Yeates, T. O. (2002) Arrangement of subunits and ordering of beta-strands in an amyloid sheet, *Nat. Struct. Biol. 9*, 734−9.
20. Olofsson, A., Ippel, H. J., Baranov, V., Horstedt, P., Wijmenga, S., and Lundgren, E. (2001) Capture of a dimeric intermediate during transthyretin amyloid formation, *J. Biol. Chem. 276*, 39592−9.
21. Olofsson, A., Ippel, J. H., Wijmenga, S. S., Lundgren, E., and Ohman, A. (2004) Probing solvent accessibility of transthyretin-amyloid by solution NMR spectroscopy, *J. Biol. Chem. 279*, 5699−5707.
22. Eneqvist, T., Andersson, K., Olofsson, A., Lundgren, E., and Sauer-Eriksson, A. E. (2000) The β-Slip: A Novel Concept in Transthyretin Amyloidosis, *Mol. Cell 6*, 1207−18.
23. Ferrao-Gonzales, A. D., Souto, S. O., Silva, J. L., and Foguel, D. (2000) The preaggregated state of an amyloidogenic protein: hydrostatic pressure converts native transthyretin into the amyloidogenic state, *Proc. Natl. Acad. Sci. U.S.A. 97*, 6445−50.
24. Sacchettini, J. C., and Kelly, J. W. (2002) Therapeutic strategies for human amyloid diseases, *Nat. Rev. Drug Discovery 1*, 267−75.
25. Hammarström, P., Wiseman, R. L., Powers, E. T., and Kelly, J. W. (2003) Prevention of transthyretin amyloid disease by changing protein misfolding energetics, *Science 299*, 713−6.
26. Cohen, F. E., and Kelly, J. W. (2003) Therapeutic approaches to protein-misfolding diseases, *Nature 426*, 905−9.
27. Ando, Y., Ohlsson, P. I., Suhr, O., Nyhlin, N., Yamashita, T., Holmgren, G., Danielsson, A., Sandgren, O., Uchino, M., and Ando, M. (1996) A new simple and rapid screening method for variant transthyretin-related amyloidosis, *Biochem. Biophys. Res. Commun. 228*, 480−3.
28. Kishikawa, M., Nakanishi, T., Miyazaki, A., Shimizu, A., Nakazato, M., Kangawa, K., and Matsuo, H. (1996) Simple detection of abnormal serum transthyretin from patients with familial amyloidotic polyneuropathy by high-performance liquid chromatography/electrospray ionization mass spectrometry using material precipitated with specific antiserum, *J. Mass Spectrom. 31*, 112−4.
29. Suhr, O. B., Ando, Y., Ohlsson, P. I., Olofsson, A., Andersson, K., Lundgren, E., Ando, M., and Holmgren, G. (1998) Investigation into thiol conjugation of transthyretin in hereditary transthyretin amyloidosis, *Eur. J. Clin. Invest. 28*, 687−92.
30. Suhr, O. B., Svendsen, I. H., Ohlsson, P. I., Lendoire, J., Trigo, P., Tashima, K., Ranlov, P. J., and Ando, Y. (1999) Impact of age and amyloidosis on thiol conjugation of transthyretin in hereditary transthyretin amyloidosis, *Amyloid: Int. J. Exp. Clin. Invest. 6*, 187−91.
31. Thylén, C., Wahlqvist, J., Haettner, E., Sandgren, O., Holmgren, G., and Lundgren, E. (1993) Modifications of transthyretin in amyloid fibrils: analysis of amyloid from homozygous and heterozygous individuals with the Met30 mutation, *EMBO J. 12*, 743−8.
32. Altland, K., Winter, P., and Sauerborn, M. K. (1999) Electrically neutral microheterogeneity of human plasma transthyretin (prealbumin) detected by isoelectric focusing in urea gradients, *Electrophoresis 20*, 1349−64.
33. Altland, K., Winter, P., Saraiva, M. J., and Suhr, O. (2004) Sulfite and base for the treatment of familial amyloidotic polyneuropathy: two additive approaches to stabilize the conformation of human amyloidogenic transthyretin, *Neurogenetics 5*, 61−7.
34. Zhang, Q., and Kelly, J. W. (2003) Cys10 mixed disulfides make transthyretin more amyloidogenic under mildly acidic conditions, *Biochemistry 42*, 8756−61.
35. Zhang, Q., and Kelly, J. W. (2005) Cys-10 Mixed Disulfide Modifications Exacerbate Transthyretin Familial Variant Amyloidogenicity: A Likely Explanation for Variable Clinical Expression of Amyloidosis and the Lack of Pathology in C10S/V30M Transgenic Mice?, *Biochemistry 44*, 9079−85.
36. Takaoka, Y., Ohta, M., Miyakawa, K., Nakamura, O., Suzuki, M., Takahashi, K., Yamamura, K., and Sakaki, Y. (2004) Cysteine 10 is a key residue in amyloidogenesis of human transthyretin Val30Met, *Am. J. Pathol. 164*, 337−45.
37. Ueno, S., Uemichi, T., Yorifuji, S., and Tarui, S. (1990) A novel variant of transthyretin (Tyr114 to Cys) deduced from the nucleotide sequences of gene fragments from familial amyloidotic polyneuropathy in Japanese sibling cases, *Biochem. Biophys. Res. Commun. 169*, 143−7.

38. Ueno, S., Fujimura, H., Yorifuji, S., Nakamura, Y., Takahashi, M., Tarui, S., and Yanagihara, T. (1992) Familial amyloid polyneuropathy associated with the transthyretin Cys114 gene in a Japanese kindred, *Brain 115*, 1275−89.
39. Haagsma, E. B., Post, J. G., DeJager, A. E. J., Nikkels, P. G. J., Hamel, B. C. J., and Hazenberg, B. P. C. (1997) A dutch kindred with familial amyloidotic polyneuropathy associated with the transthyretin Cys 114 mutant, *Amyloid: Int. J. Exp. Clin. Invest. 4*, 112−7.
40. Eneqvist, T., Olofsson, A., Ando, Y., Miyakawa, T., Katsuragi, S., Jass, J., Lundgren, E., and Sauer-Eriksson, A. E. (2002) Disulfide-bond formation in the transthyretin mutant Y114C prevents amyloid fibril formation in vivo and in vitro, *Biochemistry 41*, 13143−51.
41. Blake, C. C., Geisow, M. J., Oatley, S. J., Rérat, B., and Rérat, C. (1978) Structure of prealbumin: secondary, tertiary and quaternary interactions determined by Fourier refinement at 1.8 Å, *J. Mol. Biol. 121*, 339−56.
42. Hörnberg, A., Eneqvist, T., Olofsson, A., Lundgren, E., and Sauer-Eriksson, A. E. (2000) A Comparative Analysis of 23 Structures of the Amyloidogenic Protein Transthyretin, *J. Mol. Biol. 302*, 649−69.
43. Sauer, U. H., and Ceska, T. A. (1997) A simple method for making reproducible fibre loops for protein cryocrystallography, *J. Appl. Crystallog. 30*, 71−2.
44. Jones, T. A., Zou, J. Y., Cowan, S. W., and Kjeldgaard (1991) Improved methods for binding protein models in electron density maps and the location of errors in these models, *Acta Crystallogr. A47*, 110−9.
45. Collaborative Computational Project, N. (1994) The CCP4 suite: programs for protein crystallography, *Acta Crystallogr. D50*, 760−3.
46. Murshudov, G. N., Vagin, A. A., and Dodson, E. J. (1997) Refinement of macromolecular structures by the maximum-likelihood method, *Acta Crystallogr. D53*, 240−55.
47. Goldsteins, G., Persson, H., Andersson, K., Olofsson, A., Dacklin, I., Edvinsson, Å., Saraiva, M. J., and Lundgren, E. (1999) Exposure of cryptic epitopes on transthyretin only in amyloid and in amyloidogenic mutants, *Proc. Natl. Acad. Sci. U.S.A. 96*, 3108−13.
48. Jiang, X., Smith, C. S., Petrassi, H. M., Hammarstrom, P., White, J. T., Sacchettini, J. C., and Kelly, J. W. (2001) An engineered transthyretin monomer that is nonamyloidogenic, unless it is partially denatured, *Biochemistry 40*, 11442−52.
49. Gustavsson, A., Engstrom, U., and Westermark, P. (1991) Normal transthyretin and synthetic transthyretin fragments form amyloid-like fibrils in vitro, *Biochem. Biophys. Res. Commun. 175*, 1159−64.

BI050795S